

# Synthesis and Characterization of Green CuO using *Centella Asiatica* Plant Leaf Extract: Electrochemical and Photocatalytic Activities

K. Rudresha<sup>1,2</sup>, A. Zahir Hussain<sup>2</sup>, Ravikumar C. R.<sup>1,\*</sup>, M. R. Anil Kumar<sup>1</sup>, Nagaswarupa H. P.<sup>3</sup>, M. S. Santosh<sup>4</sup>, H. C. Ananda Murthy<sup>5,\*</sup>

<sup>1</sup>Research Centre, Department of Science, East West Institute of Technology, Bangalore 560091, Karnataka, India

<sup>2</sup>Post Graduate and Research Department of Chemistry, Jamal Mohamed College (Autonomous) Affiliated to Bharathidasan University, Tiruchirappalli 620020, Tamilnadu, India

<sup>3</sup>Department of Studies in Chemistry, Davanagere University, Shivagangothri, Davanagere 577007, Karnataka, India

<sup>4</sup>Centre for Incubation, Innovation, Research and Consultancy (CIIRC), Jyothi Institute of Technology, Bangalore 560082, Karnataka, India

<sup>5</sup>Department of Applied Chemistry, School of Applied Natural Science, Adama Science and Technology University, P.O. Box 1888, Adama, Ethiopia

\*Corresponding authors: E-mail: [ravic128@gmail.com](mailto:ravic128@gmail.com); Tel.: (+91) 9902284932 (C. R. Ravikumar)  
[anandkps350@gmail.com](mailto:anandkps350@gmail.com); Tel.: (+251) 988683640 (H. C. Ananda Murthy)

DOI: 10.5185/amlett.2020.121586

The green CuO NPs were successfully synthesised by green solution combustion method. The average crystallite size of green solution combustion CuO nanoparticles (gsc-CONPs) was found to be 40.64 nm and confirmed by powder X-ray diffraction (PXRD) analysis. The UV-DRS spectrum revealed average energy gap of 1.75 eV for gsc-CONPs. Cyclic voltammetry (CV) and Electrochemical impedance spectroscopy (EIS) techniques have been employed to analyse the electrochemical properties of the synthesized sample by using carbon paste electrodes in 1M KOH solution. The observed results suggest superior electrochemical properties of gsc-CONPs electrode due to its lower value of  $E_{O-E_R}$ . It also exhibited better sensor characteristics for paracetamol and glucose molecules. The proton diffusion coefficient (D) for the gsc-CONPs electrode material was found to be  $1.134 \times 10^{-4} \text{ cm}^2\text{s}^{-1}$ . The g-CONPs have also been tested for its photocatalytic activity using indigo carmine (IC) dye. The mechanism suggests that the crucial role was played by OH radicals during dye degradation. The results support the claim of the synthesized gsc-CONPs as a promising material for photocatalytic and supercapacitor applications.

## Introduction

Nowadays, the metal and metal oxides nanoparticles are gaining increased attention due to their distinctive properties, like improved surface area, electrical conductivity, optical property, catalytic conversion efficiency, etc. Copper oxide (CuO) is a potential p-type semiconductor with excellent optical, electrical and magnetic properties which can be tailored by synthetic methods. Consequently, it is widely used as catalysts [1], solar energy conversion [2], gas sensors [3] and field emission [4].

A knowledge on the chemical, physical, crystallization and solution chemistry of CuO compounds will be of great help for material synthesis and performance. In the past few decades, several methods such as thermal oxidation [5], sonochemical [6], combustion [7], quick-precipitation [8] and green methods [9] have been proposed to produce CuO nanoparticles (NPs) with altered sizes and shapes, viz. nanowire, nanorods, nano needle and nano-flower. Amongst these, precipitation technique has an advantage of operating at low temperature, cheap and cost-efficient for big scale production and better yield. But green synthetic is

preferred due to its simple, nontoxic and eco-friendly nature. Also, most of the green metal oxide nanoparticles are employed for biological applications. Efforts are being made to produce CuO NPs with better electrochemical and catalytic performances [10] via green solution combustion method. The *Centella asiatica* plant leaf extract has been identified for the synthesis of CuO NPs. *Centella asiatica* has been used as traditional herb. It is a native of India, Malaysia, South Africa, Sri Lanka, and Madagascar. In India, it is being used to treat diseases like skin, urethritis, asthma, bronchitis, gastric, leprosy and kidney troubles. Studies on the aerial parts of *Centella asiatica* have revealed three new compounds namely, centellin, asiaticin and centellicin. The triterpene derivatives of this plant are believed to exhibit unique electrochemical properties because of their cyclic nature of compounds.

The main objective of the present work was to synthesize green solution combustion CuO NPs (gsc-CONPs) using *Centella asiatica* plant extract. The crystal structure, optical properties, surface bonding features and morphology of the gsc-CONPs were evaluated by using PXRD, UV-DRS, FT-IR and TEM techniques respectively.

The cyclic voltammetry and electrochemical impedance spectroscopy methods were employed to analyse the electrochemical properties of the synthesized nanomaterials by using carbon paste electrodes. The photocatalytic efficiency of gsc-CuO was evaluated by using Indigo carmine dye.

## Experimental

### Preparation of CuO NPs

The CuO NPs was synthesized by using as green fuel (*Centella asiatica* plant extract) under green solution combustion method. Freshly collected 30 mL of *Centella asiatica* plant leaf extract was mixed with 70 mL of distilled water. The obtained stock solution was refrigerated at 4 °C and later used as a bio-fuel for the synthesis of CuO NPs under green solution combustion method. The metal precursors of cupric nitrate (Sigma-Aldrich) were taken in silica crucible and 10 mL of plant latex was added to each crucible. Then the reaction mixture was kept for stirring for about 5–10 min using magnetic stirrer. Blend was placed in a preheated muffle furnace maintained at  $400 \pm 10$  °C. The solution underwent self-ignition and the whole process took 5 min for completion. The precipitate so obtained was further calcined at 800 °C for 1 hour [11] to get gsc-CONPs.

### Preparation of carbon paste electrode

For the preparation of carbon paste electrode, a mixture of the prepared sample gsc-CONPs, graphite powder and silicon oil with a mass ratio of 15:70:15 was subjected to blending in the agate mortar for about 30 minutes. The obtained paste was then filled into a Teflon cavity tube fabricated for the experimental purpose. The surface of the packed carbon paste was then levelled by pressing it gently on a weighing paper [12].

## Results and discussion

### PXRD analysis

The PXRD pattern of gsc-CONPs is as shown in Fig. 1.

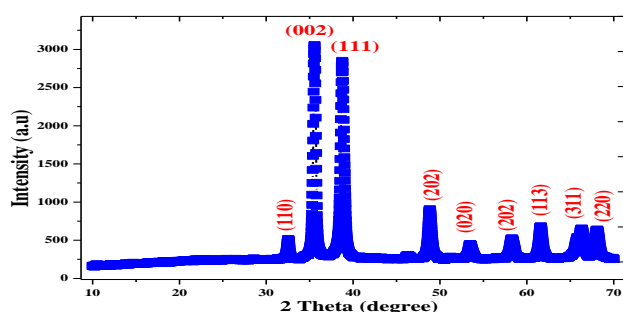


Fig.1. PXRD Pattern of gsc-CONPs.

The pattern showed a series of diffraction peaks at  $2\theta$  value of 32.58, 35.56, 38.78, 48.84, 53.41, 58.30, 61.59, 66.21 and 67.98 which were well assigned to (110), (002), (111), (202), (020), (202), (113), (311) and (220) planes. The intensities and positions of the peaks are in good agreement with literature values and is also well consistent with the JCPDS data (48-1548). The results confirmed the

single-phase and monoclinic structure of the synthesized gsc-CONPs [13].

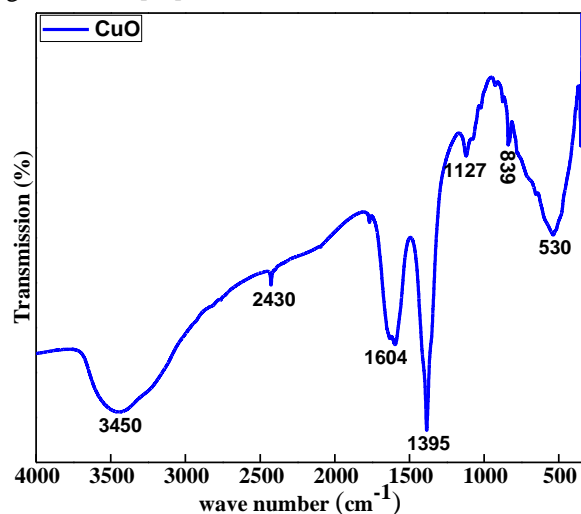


Fig. 2. FT-IR spectra of gsc-CONPs.

### FTIR studies

Fig. 2 reveals the FTIR spectrum of gsc-CONPs. The formation of CuO is confirmed by the strong band at  $530 \text{ cm}^{-1}$  which is a characteristic peak of metal (Cu)-oxygen band [14]. Further, an additional peak observed at about  $1395 \text{ cm}^{-1}$  can be assigned to  $\text{Cu}^{2+}$ - $\text{O}^{2-}$  stretching [15] whereas the band at  $839 \text{ cm}^{-1}$  corresponds to the elongation and deformation of the vibratory Cu–O band. The weak and broad absorption bands at  $1604 \text{ cm}^{-1}$  and  $3450 \text{ cm}^{-1}$  have been observed due to the presence of  $\text{H}_2\text{O}$  molecules. A sharp peak at  $2430 \text{ cm}^{-1}$  in all CuO NPs is due to the presence of atmospheric  $\text{CO}_2$ . The peaks at  $3430$  and  $1600 \text{ cm}^{-1}$  belong to stretching and bending vibration of the OH group observed in both the materials.

### UV-DRS studies

The UV-DRS and energy band gap spectra of gsc-CONPs are shown in Fig. 3. The spectrum is plotted in terms of  $F(R)$ , which is considered equivalent to the absorption coefficient. The  $\text{Cu}^{2+}$  state has a monoclinic symmetry with  $3d^9$  electronic configuration. In Fig. 3, the major absorption band appearing at 420 nm is due to the spin-allowed d–d transitions of monoclinic  $\text{Cu}^{2+}$  ions. However, the powder sample diffuses the light to a large extent making the absorption spectrum complicated to understand. To simplify, UV-DRS spectrum along with Schuster–Kubelka–Munk (SKM) relation have been utilized to correlate the diffused reflectance to absorption coefficient as given by the following equation [16, 17].

$$F(R) = \frac{(1 - R)^2}{2R} \quad (1)$$

where  $R$  is the absolute reflectance of the sample and  $F(R)$  is the Kubelka–Munk function. The optical band gap of the prepared sample was calculated using Tauc relation as in equation (2),

$$F(R)h\nu = A(h\nu - E_g)^n \quad (2)$$

where  $n = 2$  for a direct allowed transition and  $n = 1/2$  for an indirectly allowed transition,  $A$  is the constant, and  $h\nu$  is the photon energy [18,19]. Ideally, the linear portion of the curve was extrapolated to  $(F(R)h\nu)^2 = 0$  to get the direct band gap energy value of 1.75 eV as shown in Fig. 3(b).

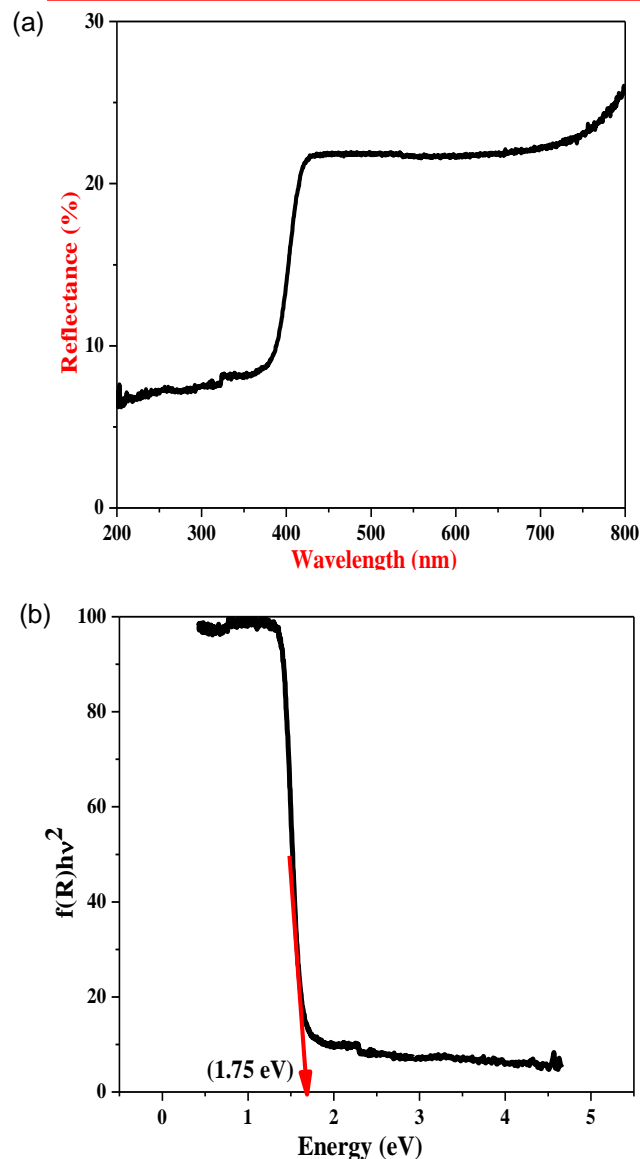


Fig. 3. (a) Diffuse reflectance spectrum of gsc-CONPs. (b) Energy gap spectrum of gsc-CONPs 3.4.

### TEM analysis

TEM micrographs of gsc-CONPs revealed crystalline nature as appeared in Fig. 4. (a, b and c). The TEM images demonstrated that the particles were spherical with an estimated range of 20 nm. The SAED pattern suggests a polycrystalline nature of the NPs as identified by some bright spots and rings. The cross section "d" spacing calculated was around 0.228 nm for the plane (111), which is in close proximity to 0.232 nm for (111) plane of CuO as reported earlier [20].

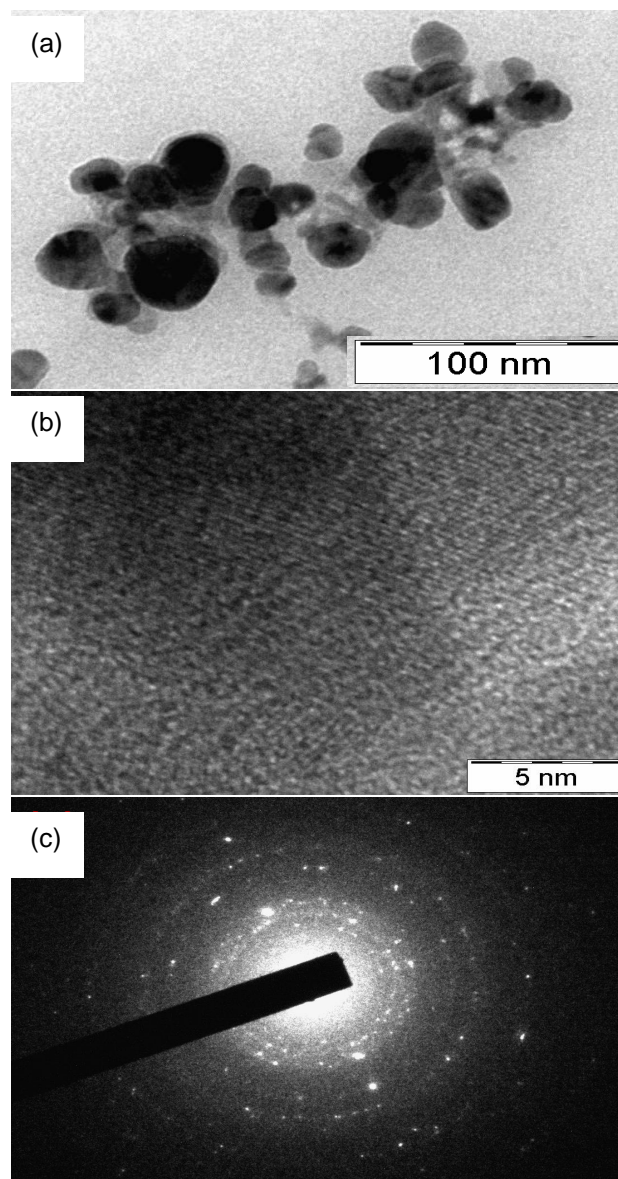


Fig. 4. TEM images of gsc-CONPs.

### Electrochemical analysis

#### Cyclic voltammetric study

Fig. 5. shows the CV spectra of gsc-CONPs studied at different scan rates. The spectra reveal the presence of redox peaks indicating a pseudo capacitance nature of the electrochemical process.

The specific capacitance of gsc-CONPs were estimated using the following equation [21],

$$C = \frac{i}{v \times m} \quad (3)$$

where  $C$  ( $\text{Fg}^{-1}$ ) is the specific capacitance,  $m$  (mg) is the mass of the active material,  $i$  (A) is the average current and  $v$  (mv/s) is the scan rate. The specific capacitance of the gsc-CONPs electrode at  $10\text{mVs}^{-1}$  was calculated to be  $262 \text{ Fg}^{-1}$ .

Further, according to the Randles-Sevcik equation [22], the peak current for a reversible process is symbolized by,

$$i_p = 2.69 \times 10^5 \times n^{3/2} \times A \times D^{1/2} \times C_0 \times v^{1/2} \quad (4)$$

where the number of electrons transferred in the reaction, electrode area, diffusion coefficient, scanning rate and initial concentration of the chemical is denoted by  $n$ ,  $A$ ,  $D$ ,  $v$ , and  $C_0$  respectively. In the present case, the initial concentration of gsc-CONPs electrode can be calculated by using equation (5),

$$C_0 = \frac{\rho}{M} \quad (5)$$

where  $\rho$  is the theoretical density and  $M$  is the molar mass of gsc-CONPs. Fig. 5(b) correlates the cathodic peak current ( $i_p$ ) with the scan rate ( $v^{1/2}$ ). The linear behavior suggests the electrode reaction of gsc-CONPs is restricted by hydrogen diffusion [19]. Using the slope of the fitted line in Fig. 5(b) and equations (4) and (5), the hydrogen diffusion coefficient ( $D$ ) for gsc-CONPs electrode was calculated to be  $1.134 \times 10^{-4} \text{ cm}^2\text{s}^{-1}$ .

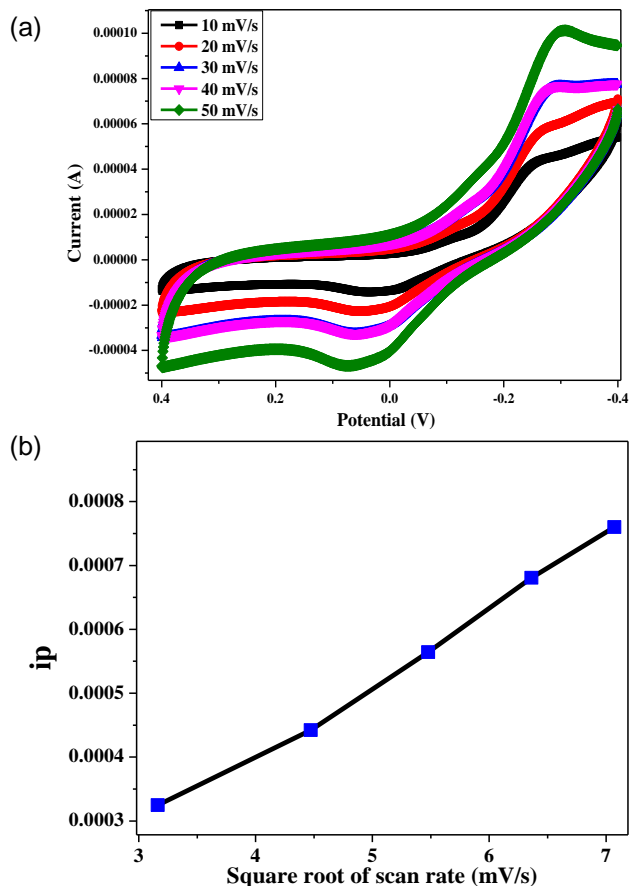


Fig. 5. (a) Cyclic voltammogram of gsc-CONPs electrode. (b) The relationship between the cathodic peak current ( $i_p$ ) and the square root of the scan rate ( $v^{1/2}$ ) for gsc-CONPs electrode.

### Electrochemical impedance analysis

Electrochemical impedance is normally measured by means of application of an AC capacity to obtain the details regarding the conductive nature of the gsc-CONPs.

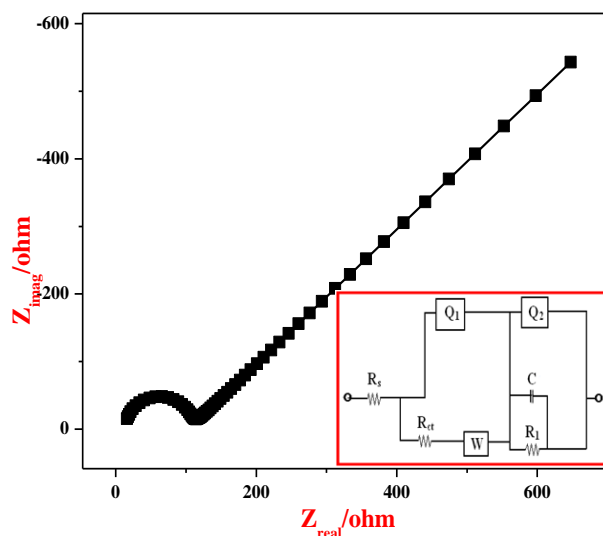


Fig. 6. The Nyquist plot and proposed equivalent circuit for gsc-CONPs electrode.

Fig. 6. shows the Nyquist plot of gsc-CONPs electrode and the corresponding equivalent circuit is given in the Inset. The Nyquist plot consists of a high-frequency region denoted by a semicircle which represents the transfer of charges occurring at the electrode/electrolyte interface and a low-frequency region signified by a straight line representing the capacitance of electrodes. The charge transfer resistance  $R_{ct}$  can be directly measured as the diameter of the semicircle arc on the real axis [23-25]. The smaller diameter of the semicircle arc represents a lower  $R_{ct}$  value for the sample. On moving further towards Y-axis, the linear curve suggests a high capacitance of the sample [26]. The ESR and charge transfer resistance  $R_{ct}$  obtained from the Nyquist plot are tabulated in Table 1.

Table 1. EIS data are for electrodes of gsc-CONPs.

Name of the electrode	Solution resistance ( $R_s$ ) ( $\Omega$ )	Charge-transfer resistance ( $R_{ct}$ ) ( $\Omega$ )	Capacitance of double layer ( $C_{dl}$ ) (F)	Constant Phase element ( $Q_1$ ) (rad/S)	Low frequency capacitance ( $Q_2$ ) (F)
gsc-CONPs	12.78	85.54	$2.408 \times 10^{-5}$	0.000454	0.000322

### Sensor application

Fig. 7. shows the cyclic voltammograms of CuO NPs, detection of glucose and paracetamol (1 mM), correspondingly. An extreme distinction of reduction and oxidation peak arrangement took place, corroborating that the synthesized carbon paste electrodes using CuO NPs derived from green synthesis method are successful material for sensing the glucose and paracetamol in alkaline medium. An anodic oxidation and cathodic reduction peaks for CuO electrode were found at  $-0.2 \text{ V}$  and  $-0.5 \text{ V}$ . However, in the cyclic voltammogram for the glucose sensing, oxidation and cathodic peaks were found in the same position but an additional peak shows in the anodic elevation at  $-0.45 \text{ V}$ . But in the sensing of the paracetamol an extra reduction peak shows at  $-0.3 \text{ V}$  with the total vanishing observed for reduction peak at  $-0.5 \text{ V}$ .

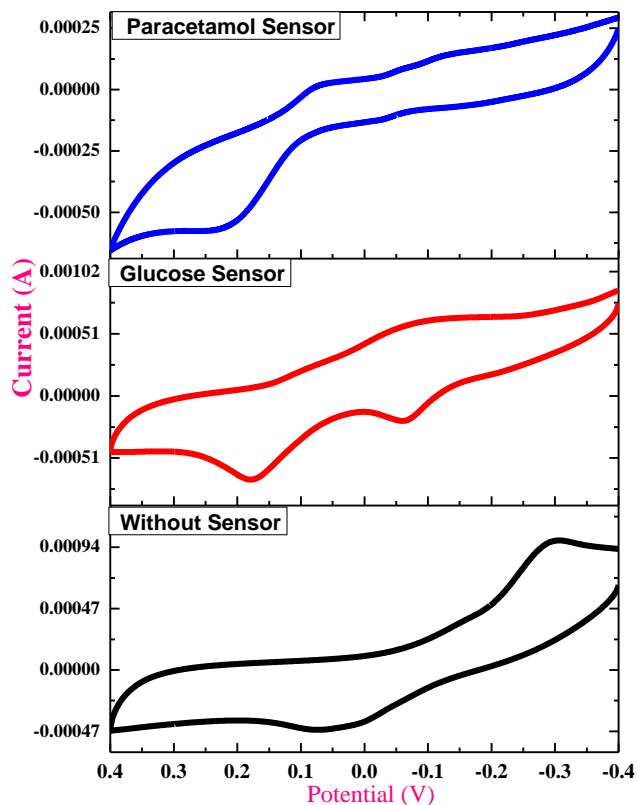


Fig. 7. Cyclic voltammogram of CuO NPs, detection of glucose and paracetamol of 1mM Concentration.

### Decolorisation of Indigo Carmine (IC)

Photocatalytic decolorisation effectiveness of gsc-CONPs was carried out on indigo carmine (IC) dye under UV light irradiation. Decolorisation rate of the dye molecules were estimated with respect to the weight of the material and concentration used. As seen from Fig. 8 the absorption peak of IC at 610 nm showed a gradual decrease with the progression in time (from 0 to 60 min) which means that gsc-CONPs were capable of IC photo-decolorisation.

The percentage degradation and kinetic parameters are presented in Table 2. The percentage of decolorisation of IC dye by gsc-CONPs by green synthesis method was found to be 92 under UV light after 60 min irradiation time. The result of the kinetic analysis, as tabulated in Table 2, suggest a pseudo-first-order kinetics for the photocatalytic reactions in line with the Langmuir–Hinshelwood model. The photocatalytic dye degradation by gsc-CONPs was found to be better compared to CuO NPs prepared by other route [27]. The high photocatalytic activity can be justified by the following (1) increase in production and transportation rate of the photogenerated electron–hole pairs (2) The green synthetic method employed would have resulted in reduction of band gap resulting in the appearance of the absorption edge in the visible light range (3) enhanced absorptivity of the IC on the catalyst surface due to the p–p interaction between the CuO and the IC molecules [28-30].

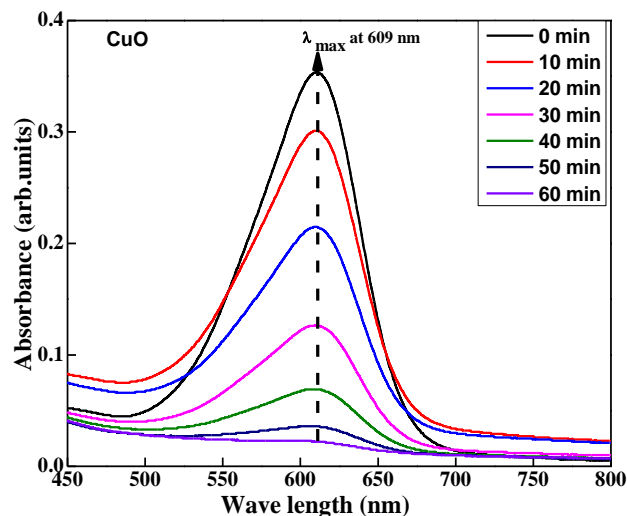


Fig. 8. Absorbance spectra of Indigo Carmine (IC) for CuO under UV light irradiation.

Table 2. Rate constants and Kinetic studies of gsc-CONPs for the decolorization of Indigo Carmine (IC) under UV light.

(A) 20PPM IC + 60mg CuO GREEN+UV					
t	c	c/c <sub>0</sub>	log c/c <sub>0</sub>	-log c/c <sub>0</sub>	%D
0	20	1	0	0	0
10	11.44	0.572	-0.2426	0.242604	42.8
20	11	0.55	-0.25964	0.259637	45
30	10.24	0.512	-0.29073	0.29073	48.8
40	5.57	0.2785	-0.55517	0.555175	72.15
50	2.86	0.143	-0.84466	0.844664	85.7
60	1.74	0.087	-1.06048	1.060481	92
			Slope	<b>0.014835</b>	
			Rate	<b>0.034164</b>	

### Conclusion

In this study, CuO were synthesized by green solution combustion method. The prepared CuO nano-material is monoclinic in structure with a band gap of 1.75 eV. The results obtained from CV and EIS confirm the superior electrochemical properties of the CuO NPs. The proton diffusion coefficient (D) for the CuO electrode material was found to be  $1.134 \times 10^{-4} \text{ cm}^2\text{s}^{-1}$ . The sample has low resistance and high capacitance making it suitable for capacitance applications. Also, the CuO can be easily made into steady electrode materials to check oxidation–reduction of glucose or paracetamol. Simultaneously, the synthesized CuO NPs also has the ability of photocatalytic dye degradation as observed by the studies conducted on IC dye. This potential can be further exploited for the degradation of several other dyes and organic pollutants present in waste water.

### Acknowledgements

Authors KR, MRA, CRR wish to thank VGST, Govt. of Karnataka, India, (No: VGST/CISEE/2014-15/282) and (VGST/K-FIST-L1/2014-15/GRD-360) for extending their support to carry out this research work and Adama Science and Technology University, Ethiopia.

#### Author's contributions

Rudresha, Zahir, Ravikumar: Conceived and designed the experiments; Performed the experiments.  
Anilkumar, Shashishekar, Santhosh and Ananda Murthy: Analysed and interpreted the data; Contributed reagents, materials, analysis tools or data; Wrote the paper.

#### Conflicts of interest

The authors declare that they have no conflicts of interest

#### Keywords

Green CuO NPs, Proton diffusion co-efficient, dye degradation, photocatalysts, electrochemical studies.

Received: 17 June 2020

Revised: 27 June 2020

Accepted: 03 September 2020

#### References

1. Jianliang, C.Y.; Tianyi, W, Yuping; Liu M.; Zhongyong, Y.; *J. Nat. Gas. Chem.*, **2011**, *20*, 669.
2. Jess, K.; Nicolas, G.; Richard, R.; Miller, E.; *Sol. Energy Mater. Sol. Cells.*, **2009**, *94*, 12.
3. Murthy, Murthy, H.C.A.; Tegene, D.Z.; Abebe, B.; *Mat. Res. Express*, **2020**, *7*, 5.
4. Murthy, H.C.A.; Tegene, D.Z.; Kasa, M; Abebe, B.; Assefa, T.; *J. Nanomater.*, **2020**, *1*.
5. Manmeet, K.; Mutha, K.P.; Deshpande, S.K.; Shipra, C.; Neetika, J.B.V.; Gupta, S.K.; Yakhmi, J.V.; *J. Cryst. Growth*, **2011**, *289*, 670.
6. Narongdet, W.; Piyanut, C.; Naratip, V.; Wisanu, P.; *Energy Procedia*, **2011**, *29*, 404.
7. Yamukyan, M.H.; Manukyan, K.V.; Kharatyan, S.L.; *Chem. Eng. J.*, **2008**, *137*, 636.
8. Zhu, J.; Li, D.; Chen, H.; Yang, X.; Lu, L.; Wang, X.; *Mater. Lett.*, **2004**, *58*, 3324.
9. Murthy, H.C.A.; Abebe, B.; Tegene, D.Z.; *Mat. Sci. Res. Ind.* **2018**, *15*, 279.
10. Le, M.; Ren, M.; Zhang, Z.; Sprunger, P.T.; Kurtz, R.L.; Flake, J.C.; *J. Electrochem. Soc.*, **2011**, *158*, 45.
11. Murthy, H.C.A.; Arun kumar, N.B.; Sirajuddin; J. Nagaswarupa H P; Ravikumar, C R; Anil Kumar M R; *Adv. Mater. Lett.*, **2020**, *11*, 1.
12. Anil Kumar, C.R.; Ravikumar, Nagaswarupa, H.P.; Purshotam, B.; Bedasa A.G.; Murthy, H.C.A.; Fedlu, K.S.; Samson, T.; *J. Environ. Chem. Engg.*, **2019**, *7*, 103468.
13. Ethiraj, A.S.; Kang, D.J.; *Nanoscale. Res. Lett.*, **2012**, *7*, 70.
14. Liu, J.; Huang, X.; Li, Y.; Sulleman, K.; He, X.; Sun, F.; *J. Mater. Chem.*, **2006**, *16*, 4427.
15. Prakash, V.; Diwan, R.K.; Niyogi, U.K.; *Indian J. Pure Appl. Phys.*, **2015**, *53*, 753.
16. Jisha, P.K.; Ramachandra, N.; Prashantha, S.C.; Ravikumar, C.R.; Nagaswarupa, H.P.; Nagabhushana, H.; Jnaneshwara, D.M.; *Materials Today: Proceedings*, **2017**, *4*, 11706.
17. Ravikumar, C.R.; Kotteeswaran, P.; Murugan, A.; Bheemaraju, V.; Santosh, M.S.; Nagaswarupa, H.P.; Nagabhushana, H.; Prashantha, S.C.; Anil Kumar, M.R.; Gurushantha, K.; *Materials Today: Proceedings*, **2017**, *4*, 12205.
18. Arun kumar, N.B.; Sirajudeen, J.; Nagaswarupa, H.P.; Prashantha, S.C.; Anil Kumar, M.R.; Ravikumar, C.R.; Gurushantha, K.; Shashishekar, T.R.; Anantharaju, K.S.; Nagabhushana, H.; Sharma, S.C.; *Materials Today: Proceedings*, **2017**, *4*, 11827.
19. Ravikumar, C.R.; Kotteeswaran, P.; Bheemaraju, V.; Murugan, A.; Santosh, M.S.; Nagaswarupa, H.P.; Prashantha, S.C.; Anil kumar, M.R.; Shivakumar, M.S.; *J. Energy Storage*, **2017**, *9*, 12.
20. Avinash, B.; Ravikumar, C.R.; Anil Kumar, M.R.; Nagaswarupa, H.P.; Santosh, M.S.; Aarti Bhatt, S.; Denis, K.; *J. Phys. Chem. Solids*, **2019**, *134*, 193.
21. Ravikumar, C.R.; Santosh, M.S.; Nagaswarupa, H.P.; Prashantha, S.C.; Yallappa, S.; Anil Kumar, M.R.; *Mater. Res. Express.*, **2017**, *4*, 065503.
22. Ravikumar, C.R.; Anil Kumar, M.R.; Nagaswarupa, H.P.; Prashantha, S.C.; Bhatt, A.S.; Santosh, M.S.; Kuznetsov, D.; *J. Alloys. Compd.*, **2018**, *738*, 332.

23. Raveesha, H.R.; Nayana, S.; Vasudha, D.R.; Shabaaz, B.J.P.; Pratibha, S.; Ravikumar, C.R.; Dhananjay, N.; *J. Science: Advanced Materials and Devices*, **2019**, *4*, 57.
24. Anil Kumar, M.R.; Nagaswarupa, H.P.; Ravikumar, C.R.; Prashantha, S.C.; Nagabhushana, H.; Aarti Bhatt, S.; *J. Phys. Chem. Solids*, **2019**, *127*, 127.
25. Shruthi, B.; Madhu, B.J.; Bheemaraju, V.; Vynatheya, S.; Veena Devi, B.; Jayashree, G.V.; Ravikumar, C.R.; *J. Science: Advanced Materials and Devices*, **2017**, *2*, 93.
26. Girish, K.M.; Prashantha, S.C.; Nagabhushana, H.; Ravikumar, C.R.; Nagaswarupa, H.P.; Ramachandra, N.; Premakumar, H.B.; Umesh, B.; *J. Science: Advanced Materials and Devices*, **2018**, *3*, 151.
27. Ebrahim, S. M.; Mina, S.; Ali, R.; Saeid, T.F.; *J. Mater. Sci.: Mater. Electron*, **2018**, *29*, 1333.
28. Yang, J.; Zhao, X.; Fan, H.; Yang, L.; Zhang, Y.; Li, X.; *J. Alloys. Compd.*, **2013**, *556*, 1.
29. Abebe, B.; Murthy, H.C.A.; Amare, E.Z.; Adimasu, Y.; *Inorg. Nano-Metal Chem.*, **2020**, 1–12.
30. Anil Kumar, M.R.; Abebe, B.; Nagaswarupa, H.P.; Murthy, H.C.A.; Ravikumar, C.R.; Fedlu, K.S.; *Sci. Rep.*, **2020**, *10*, 1249.

#### Authors biography



Dr. H. C. Ananda Murthy has been a dedicated faculty member at various prestigious universities in India, Tanzania and Ethiopia for the last 23 years. He is currently working as Associate Professor, Department of Applied Chemistry, Adama Science and Technology University, Adama, Ethiopia, East Africa. Prof. Ananda has published more than 50 research articles in the journals of international repute and authored 5 books, 3 book chapters & 6 compendia. He has taught various chemistry courses to UG, PG, and Ph.D. students of the universities. His research interest mainly includes synthesis and applications of composite materials and Nano-materials. He is currently associated with research projects related to green synthesis of metal and metal oxide nanoparticles for multifunctional applications.



Dr. Ravikumar C.R. is a committed faculty member working as Associate Professor in Chemistry, East West Institute of Technology, Bangalore, India. He has published more than 50 papers in journal of high reputation and presented many papers in conferences. His research interest include electrochemistry, batteries and photocatalysis. He has involved in many research projects and supervisor for PhD students.